

Received 7 March 2024, accepted 26 March 2024, date of publication 29 March 2024, date of current version 4 April 2024.

Digital Object Identifier 10.1109/ACCESS.2024.3382996

RESEARCH ARTICLE

Cooperative Control of TSO and DSO: Management of Line Congestion and Frequency Response

KIPO YOON¹, (Member, IEEE), JOOHYUK LEEM¹, (Student Member, IEEE),
SOO HYOUNG LEE², (Member, IEEE), AND JUNG-WOOK PARK¹, (Senior Member, IEEE)

¹School of Electrical and Electronic Engineering, Yonsei University, Seoul 03722, South Korea

²Division of Electrical, Electronic and Control Engineering, Kongju National University, Cheonan-si 31080, South Korea

Corresponding authors: Soo Hyoung Lee (lsh@kongju.ac.kr) and Jung-Wook Park (jungpark@yonsei.ac.kr)

This work was supported by the National Research Foundation (NRF) funded by the Ministry of Science and Information and Communication Technology (MSIT), South Korea, under Grant 2020R1A3B2079407.

ABSTRACT The separation of transmission and distribution systems raises a variety of questions concerning the integration of many distributed generators (DGs) into future grids. They are difficult to solve by using current energy management methods. Especially, the cooperative control between transmission system operator (TSO) and distribution system operator (DSO) has been increasingly emphasized to manage the line congestion. This paper proposes a new cooperative control of TSO-DSO based on the generation-load power sensitivity analysis. To minimize the required computational effort and data communication, the information of TSO and DSO is processed separately in the generation-load power sensitivity matrix of power system. The proposed cooperative control is implemented by three-step process, which is aggregation, specification, and local distribution. Firstly, the DSOs aggregate the flexibility area of DGs in their networks, and they inform the TSO of the feasible operation regions (FORs). Then, the TSO sends the power references at the boundary buses to many DSOs. Thereafter, the DSOs use these references as loads to calculate the detailed power references for their generators. As the result, the net power of DSOs satisfies the power references requested by the TSO. The case studies are carried out to verify the effectiveness of proposed control. The results show that when the load is increased by 20%, the overall average of line loading is decreased by 4.34% with the proposed control. Also, when the generator of 634 MW is disconnected, the frequency nadir is increased by 0.1 Hz compared with the P - f droop control.

INDEX TERMS Cooperative control, distributed generator, distribution system operator, flexibility, frequency response, line congestion, transmission system operator.

I. INTRODUCTION

A. MOTIVATION AND INCITEMENT

Recently, worldwide attention is being focused on environmental concerns in the aftermath of the COVID-19 pandemic [1]. In this situation, more than 70 countries have pledged to achieve net zero by 2050 [2]. They include the biggest emitters that cover 76% of global emissions, such as China, United States, India, and the European Union [3]. As a part of 'Net-Zero 2050', power systems continue to increase their reliance on renewable energy generation. The

The associate editor coordinating the review of this manuscript and approving it for publication was Peter Palensky¹.

governments of major developed countries are giving strength to this movement while promoting the rapid expansion of distributed generators (DGs) [4]. However, there is no perfect solution at this moment to achieve the high penetration of renewables into power systems. In other words, the expansion of DGs raises many questions about the operational stability and reliability of power system [5].

B. LITERATURE REVIEW

Recent studies report the importance of interactions between transmission and distribution systems, where many DGs are located. In particular, they emphasize the cooperation

between transmission system operator (TSO) and distribution system operator (DSO). The main objective of cooperation is the congestion management of system with many DGs [6]. To do so, the DSO must not only make a market clearing price, but also give its proper operating points based on the feasible operation regions (FORs) calculated by the aggregation of flexibilities of DGs. This role of DSO is the most important for distribution systems because it is difficult to effectively process all real-time information of large-scale power systems at once. For the adequate support tools of preventive operation and management, it is reported in [6] that the DSO must take the advantage of power flexibility of DG not only for solving the potential line congestion and frequency problems, but also for dealing with the uncertain and variable power generation in a power system. In [7], it is required for the DSOs to distribute the DGs because the decentralized market framework to consider loss allocation and its impact on the market outcome is not compatible with the current market structures. Also, [8] describes the existence of flexibility markets or flexibility contracts, where the DSO can be an active player by purchasing or requiring flexibility volumes for the main role of DSO. Moreover, it is reported in [9] that the demand response aggregators are market participants in Finland, and the only DSOs are allowed to provide unlimited aggregator access to the smart meters. In [10] and [11], the synchronous power stations have historically provided ancillary services to the TSOs for the reliable and secure power system. However, because the DGs are largely present in distribution systems nowadays, the new ancillary services like congestion management are also required for the DSOs by enhancing the cooperative coordination between TSO and DSOs.

Many studies for the cooperation between TSO and DSO, [12], [13], [14], [15], [16], [17], [18] have covered the issues related to optimal power flow, unit commitment, economic dispatch, contingency analysis, distributed restoration, and assessment of stability and reliability, etc. Nowadays, the DSO must take advantage of the power flexibility of DG to meet these requirements by handling the aggregation of flexibilities properly. Furthermore, the methods to accurately dispatch the powers from generators to distribution networks are presented in some studies based on the use of FOR. However, there are very few studies dealing with system frequency stabilities, which is also important for operating both TSO and DSO systems. For example, the method to find the optimal market price was studied with TSO-DSO coordination in [7] and [19]. That is, the framework of market participation was presented in [7] with the generators in both the TSO and DSO. Parallel computing was used to find the market price via optimal power flow in [19]. However, they did not consider the flexibility of DGs. In [20], the random sampling method was presented to calculate the FOR. However, it did not describe how to dispatch the powers from DGs based on the result of FOR calculation. In [21], the method for finding the market price was proposed by using the statistical learning. In [22], the cost-optimal disaggregation of

FOR was presented by calculating the FOR based on the Minkowski sum. However, they did not make the analysis for the impact on improving the system response. In [23], the method for deriving the aggregated var capability curve at TSO-DSO interface was proposed. The impact of aggregated DER var support on grid voltages was analyzed when the line contingency occurs. However, the computational burden of method was not considered. In [24], the look-ahead multi-interval framework was used for the TSO-DSO operational coordination and the voltage and congestion problems were successfully solved.

The comparison of the proposed and other TSO-DSO cooperation methods is summarized in Table 1. In summary, the calculation of FOR has not been considered in some of the studies about the cooperative control of TSO-DSO. Moreover, there are not many TSO-DSO studies verifying the effectiveness to improve the frequency response. Also, analyzing the computational burden of cooperation between TSO and DSO is an important issue for the communication between them, but there are less studies calculating the computational or communicational burden of their control methods.

C. CONTRIBUTION AND PAPER ORGANIZATION

This paper proposes the new cooperative control of TSO-DSO based on generation-load power sensitivity analysis. First, the DSOs provide the FORs of their networks to the TSO by using Minkowski sum. Then, the TSO calculates the power references for the DSO. Next, the DSO calculates the detailed power references for the DGs. This enables the net power of DSOs to satisfy the power references required by the TSO while avoiding the huge additional computational resources. Moreover, the proposed cooperative control of TSO-DSO enhances the dynamic system response by allocating powers effectively. The major contributions of this paper are summarized as follows:

- By applying the generation-load power sensitivity analysis, the powers between the generators (including DGs) are allocated properly and effectively.
- The proposed cooperative control of TSO-DSO manages the line congestion and improves the frequency response of system effectively.
- The proposed approach can effectively reduce the computational burden required for the cooperative control between TSO and DSOs when compared to a centralized control approach.

The paper is organized as follows. Section II explains the details of proposed cooperative control of TSO-DSO based on the generation-load power sensitivity. In particular, the computational complexity analysis by the proposed cooperative control is carefully made. Then, Section III verifies the effectiveness of proposed cooperative control with case studies by using the DIGSILENT PowerFactory® software. Finally, conclusions are addressed in Section IV.

TABLE 1. Comparison of TSO-DSO cooperation methods.

Algorithm	Consideration of DG Flexibility	Calculation of FOR	Method for DG dispatch	Improvement of system response	Consideration of complexity
Diagonal quadratic approximation [19]	No	No	Optimal power flow	No	No
Random sampling [20]	Yes	Random sampling, optimal power flow	No	No	No
Contextual price-aware approach [21]	Yes	No	Statistical learning	No	No
Cost-optimal flexibility disaggregation [22]	Yes	Minkowski sum	Cost-optimal disaggregation	No	No
Var capability estimation [23]	Yes	Optimal power flow	Optimal power flow	Voltage	No
Look-ahead multi-interval framework [24]	Yes	No	Look-ahead multi-interval framework	Line congestion and voltage	Yes
Generation-load power sensitivity (Proposed method)	Yes	Minkowski sum	Power sensitivity analysis	Line congestion and frequency	Yes

II. PROPOSED COOPERATIVE CONTROL OF TSO-DSO
A. GENERATION-LOAD POWER SENSITIVITY ANALYSIS

The generation-load power sensitivity analysis [25] can be used to effectively and operate the power system with the high penetration of renewables by adaptively allocating the real and reactive powers to many DGs. The generation-load power sensitivity is initially derived from the power flow analysis. For power system with n buses, the active and reactive powers at bus i are calculated as

$$P_i = \sum_{j=1}^n |V_i| |V_j| |Y_{ij}| \cos(\theta_{ij} - \delta_i + \delta_j), \quad (1)$$

$$Q_i = \sum_{j=1}^n |V_i| |V_j| |Y_{ij}| \sin(\theta_{ij} - \delta_i + \delta_j), \quad (2)$$

where P_i and Q_i are the active and reactive powers at bus i . V_i and V_j are the voltage magnitudes at buses i and j , respectively. δ_i and δ_j are the voltage phase angles at buses i and j , respectively. Also, $|Y_{ij}|$ and θ_{ij} are the magnitude and angle of admittance matrix element between buses i and j , respectively. By expanding (1) and (2) based on the Taylor expansion, the general power flow analysis can be formulated as

$$\begin{bmatrix} \Delta\delta_2 \\ \vdots \\ \Delta\delta_m \\ \vdots \\ \frac{\Delta\delta_n}{\Delta V_2} \\ \vdots \\ \Delta V_m \\ \vdots \\ \Delta V_n \end{bmatrix} = \begin{bmatrix} \mathbf{J}^{P\delta} & \mathbf{J}^{PV} \\ \mathbf{J}^{Q\delta} & \mathbf{J}^Q \end{bmatrix}^{-1} \cdot \begin{bmatrix} \Delta P_2 \\ \vdots \\ \Delta P_m \\ \vdots \\ \frac{\Delta P_n}{\Delta Q_2} \\ \vdots \\ \Delta Q_m \\ \vdots \\ \Delta Q_n \end{bmatrix}, \quad (3)$$

where n is the number of buses in power system, and m is the number of DG buses. The Jacobian matrix \mathbf{J} is composed of the sub-matrices $\mathbf{J}^{P\delta}$, \mathbf{J}^{PV} , $\mathbf{J}^{Q\delta}$, and \mathbf{J}^{QV} , which are the partial derivatives of real and reactive powers with respect to the phase angles and magnitudes of bus voltages, respectively. However, there might be cases that \mathbf{J} is singular or near singular, and the power flow solution cannot be obtained by using (3), although the systems are still solvable [26]. Therefore, the equation (3) is modified by (4) with Levenberg-Marquardt method [27] as

$$\begin{bmatrix} \Delta\delta_2 \\ \vdots \\ \Delta\delta_m \\ \vdots \\ \frac{\Delta\delta_n}{\Delta V_2} \\ \vdots \\ \Delta V_m \\ \vdots \\ \Delta V_n \end{bmatrix} = \underbrace{\left[\mathbf{J}^T \mathbf{J} + \lambda \text{diag}(\mathbf{J}^T \mathbf{J}) \right]^{-1}}_{\mathbf{K}} \cdot \mathbf{J}^T \cdot \begin{bmatrix} \Delta P_2 \\ \vdots \\ \Delta P_m \\ \vdots \\ \frac{\Delta P_n}{\Delta Q_2} \\ \vdots \\ \Delta Q_m \\ \vdots \\ \Delta Q_n \end{bmatrix}, \quad (4)$$

where λ is damping factor. Note that λ is zero when \mathbf{J} is not singular, and therefore the system is well-conditioned. Otherwise, λ with small positive constant is chosen (i.e., $\lambda > 0$) to solve the power flow equation. Then, the matrix \mathbf{K} is defined as

$$\mathbf{K} = \begin{bmatrix} \mathbf{K}^{\delta P} & \mathbf{K}^{\delta P} \\ \mathbf{K}^{VP} & \mathbf{K}^{VQ} \end{bmatrix}$$

$$= \begin{bmatrix} K_{2,2}^{\delta P} & \cdots & K_{2,n}^{\delta P} & K_{2,2}^{\delta Q} & \cdots & K_{2,n}^{\delta Q} \\ \vdots & \ddots & \vdots & \vdots & \ddots & \vdots \\ K_{n,2}^{\delta P} & \cdots & K_{n,n}^{\delta P} & K_{n,2}^{\delta Q} & \cdots & K_{n,n}^{\delta Q} \\ \hline K_{2,2}^{VP} & \cdots & K_{2,n}^{VP} & K_{2,2}^{VQ} & \cdots & K_{2,n}^{VQ} \\ \vdots & \ddots & \vdots & \vdots & \ddots & \vdots \\ K_{n,2}^{VP} & \cdots & K_{n,n}^{VP} & K_{n,2}^{VQ} & \cdots & K_{n,n}^{VQ} \end{bmatrix} \quad (5)$$

where $\mathbf{K}^{\delta P}$, $\mathbf{K}^{\delta Q}$, \mathbf{K}^{VP} , and \mathbf{K}^{VQ} are submatrices. Note that the power mismatches in the right-hand side of (4) can be separated into generation and load mismatches. As the result, the phase angle and voltage magnitude mismatches in DG buses can be re-formulated as

$$\begin{bmatrix} \Delta\delta_2 \\ \vdots \\ \Delta\delta_m \\ \Delta V_2 \\ \vdots \\ \Delta V_m \end{bmatrix} = \mathbf{K}^{sq} \cdot \begin{bmatrix} \Delta P_{2G} \\ \vdots \\ \Delta P_{mG} \\ \Delta Q_{2G} \\ \vdots \\ \Delta Q_{mG} \end{bmatrix} + \mathbf{K}^{row} \cdot \begin{bmatrix} -\Delta P_{2L} \\ \vdots \\ -\Delta P_{mL} \\ \Delta P_n \\ -\Delta Q_{2L} \\ \vdots \\ -\Delta Q_{mL} \\ \vdots \\ \Delta Q_n \end{bmatrix}, \quad (6)$$

where P_{iG} and Q_{iG} are the real and reactive powers provided from DG bus i , respectively. P_{iL} and Q_{iL} are the real and reactive power consumptions in bus i , respectively. Also, the dimensions of \mathbf{K}^{sq} and \mathbf{K}^{row} are $2(m-1) \times 2(m-1)$ and $2(m-1) \times 2(n-1)$, respectively, and they are given as

$$\mathbf{K}^{sq} = \begin{bmatrix} K_{2,2}^{\delta P} & \cdots & K_{2,m}^{\delta P} & K_{2,2}^{\delta Q} & \cdots & K_{2,m}^{\delta Q} \\ \vdots & \ddots & \vdots & \vdots & \ddots & \vdots \\ K_{m,2}^{\delta P} & \cdots & K_{m,m}^{\delta P} & K_{m,2}^{\delta Q} & \cdots & K_{m,m}^{\delta Q} \\ \hline K_{2,2}^{VP} & \cdots & K_{2,m}^{VP} & K_{2,2}^{VQ} & \cdots & K_{2,m}^{VQ} \\ \vdots & \ddots & \vdots & \vdots & \ddots & \vdots \\ K_{m,2}^{VP} & \cdots & K_{m,m}^{VP} & K_{m,2}^{VQ} & \cdots & K_{m,m}^{VQ} \end{bmatrix}, \quad (7)$$

$$\mathbf{K}^{row} = \begin{bmatrix} K_{2,2}^{\delta P} & \cdots & K_{2,n}^{\delta P} & K_{2,2}^{\delta Q} & \cdots & K_{2,n}^{\delta Q} \\ \vdots & \ddots & \vdots & \vdots & \ddots & \vdots \\ K_{m,2}^{\delta P} & \cdots & K_{m,n}^{\delta P} & K_{m,2}^{\delta Q} & \cdots & K_{m,n}^{\delta Q} \\ \hline K_{2,2}^{VP} & \cdots & K_{2,n}^{VP} & K_{2,2}^{VQ} & \cdots & K_{2,n}^{VQ} \\ \vdots & \ddots & \vdots & \vdots & \ddots & \vdots \\ K_{m,2}^{VP} & \cdots & K_{m,n}^{VP} & K_{m,2}^{VQ} & \cdots & K_{m,n}^{VQ} \end{bmatrix}. \quad (8)$$

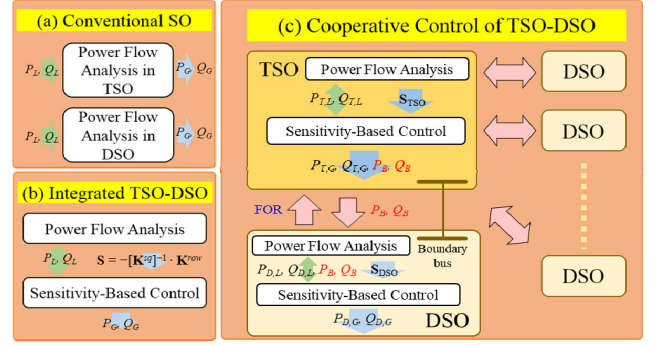


FIGURE 1. Three operations of power system: (a) conventional operation, (b) integrated TSO-DSO operation based on the generation-load power sensitivity, (c) the proposed cooperative control of TSO-DSOs.

Then, the sensitivity matrix \mathbf{S} is finally derived as

$$\begin{bmatrix} \Delta P_{2G} \\ \vdots \\ \Delta P_{mG} \\ \Delta Q_{2G} \\ \vdots \\ \Delta Q_{mG} \end{bmatrix} = \underbrace{-[\mathbf{K}^{sq}]^{-1} \cdot \mathbf{K}^{row}}_{\mathbf{S}} \cdot \begin{bmatrix} -\Delta P_{2L} \\ \vdots \\ -\Delta P_{mL} \\ \Delta P_n \\ -\Delta Q_{2L} \\ \vdots \\ -\Delta Q_{mL} \\ \vdots \\ \Delta Q_n \end{bmatrix}, \quad (9)$$

$$\mathbf{S} = \begin{bmatrix} \mathbf{S}^{11} & \mathbf{S}^{12} \\ \mathbf{S}^{21} & \mathbf{S}^{22} \end{bmatrix} = -[\mathbf{K}^{sq}]^{-1} \cdot \mathbf{K}^{row}, \quad (10)$$

where \mathbf{S}^{11} , \mathbf{S}^{12} , \mathbf{S}^{21} , and \mathbf{S}^{22} are $(m-1) \times (n-1)$ submatrices. Note that if all DG buses specify the phase angle and magnitude of voltage as physical slack bus, the term in left-hand side of (6) becomes zero. More details about the generation-load power sensitivity analysis are given in [25].

B. COOPERATIVE CONTROL OF TSO-DSO BASED ON POWER SENSITIVITY ANALYSIS

The conventional power flow analysis has been separately applied into transmission and distribution systems, as shown in Fig. 1(a), because of their huge size. In other words, the TSO operates the power system without any information from the DSOs. For this case, the distribution network is modeled as a load injection, which is estimated from its substation. Likewise, the DSOs mostly operate their networks without the close interactions with the TSO. Therefore, the transmission system is modelled by the voltage source, which is measured at the substation. In summary, the TSO and DSO are blind to each other for their operations by the conventional methods [15].

However, when the penetration of renewables in distribution systems is becoming high, it will be no longer possible to simplify the impact of DSOs on the TSO as a load

injection. Thus, the cooperative control between the TSO and DSOs becomes one of the most important issues. The sensitivity-based analyses are able to contribute to the effective integration of TSO-DSO, as shown in Fig. 1(b). However, its implementation is not easy. For example, even though there are both integral parts of interconnected power systems, they are reluctant to share their sensitive system data [19]. Thus, a central scheduling framework in Fig. 1(b), where all TSOs and DSOs share the system information, may not be proper for their entire operation [28]. Moreover, even if all TSOs and DSOs share their data, the large computational effort is required to solve the power flow problem.

In other words, the Jacobian matrix of overall system becomes much larger than that obtained in the case of Fig. 1(a). As the result, it makes more difficult to find the optimal power allocation between the generators by using the generation-load power sensitivity analysis.

To handle this, the proposed cooperative control of TSO-DSO applies the generation-load power sensitivity analysis independently to each TSO and DSO in single group, as shown in Fig. 1(c). The TSO has the sensitivity matrix, \mathbf{S}_{TSO} , which is the submatrix of \mathbf{S} containing the buses of transmission system and the boundary buses. Likewise, each DSO has its sensitivity matrix, \mathbf{S}_{DSO} , which is another submatrix of \mathbf{S} including the buses of each distribution network and boundary bus. Firstly, the DSOs aggregate the flexibility areas of DGs to determine their FORs, and they provide this FOR information to the TSO. Then, the TSO calculates the power references at the boundary buses, which are P_B and Q_B , with \mathbf{S}_{TSO} . Thereafter, the TSO sends them to the DSOs. Finally, each DSO handles them as virtual loads to compute the proper power references for the DGs with P_B , Q_B , and \mathbf{S}_{DSO} . As the result, the DSOs can effectively distribute the power generations of the DGs in response to any contingencies causing the power imbalances.

C. IMPLEMENTATION OF PROPOSED COOPERATIVE CONTROL

As shown in Fig. 2, the proposed cooperative control is implemented by three-step process, which is the bottom-up aggregation ([20], [22], [28], [29]), top-down specification, and local distribution. The first step of bottom-up aggregation (as shown in Fig. 2(a)) is to collect the flexibility areas of all DGs in a distribution system. Note that each DG is a flexible power generation unit, and it is decentralized from the grid. Then, each of the flexibility polygons is divided into five types [30], [31], [32] depending on the different types of generators and loads, as shown in Fig. 3.

Most DGs have the uncertain deviations in the power output due to continuous changes in wind conditions, solar irradiation, or load fluctuations. Therefore, this uncertainty can be considered when the FOR is calculated. In this paper, the chance-constraints are used to allow the DSOs to adjust the level of conservatism in the FOR model [33]. To this end, the chance-constrained expression for the i -th DG power

output can be defined as

$$P\{(p_i + \lambda_i, q_i) \in F_i\} \leq 1 - \varepsilon \quad (11)$$

where p_i and q_i are the forecasted real and reactive output of i -th DG, respectively, F_i is the set of i -th DG flexibility, $(1-\varepsilon)$ is the desired constraint satisfaction probability, $P\{\cdot\}$ is the transformation of inequality constraint into a chance constraint, and λ_i is the uncertainty margin to tighten the original constraint [34]. With the consideration of uncertainty, each DSO calculates the FOR, which includes the grid operating points observed at the TSO-DSO interconnection point. Then, the DSO sends the FOR information to the TSO so that the TSO can compute the required power references based on the sensitivity analysis.

In the second step of top-down specification (as shown in Fig. 2(b)), the TSO effectively allocates powers between the generators installed in the transmission system and boundary buses in response to any power imbalances. By modifying (9), this is achieved as

$$\begin{bmatrix} \Delta \mathbf{P}_{T,G} \\ \Delta \mathbf{P}_B \\ \Delta \mathbf{Q}_{T,G} \\ \Delta \mathbf{Q}_B \end{bmatrix} = \mathbf{S}_{\text{TSO}} \cdot \begin{bmatrix} \Delta \mathbf{P}_{T,L} \\ \Delta \mathbf{Q}_{T,L} \end{bmatrix}, \quad (12)$$

where the subscripts, (T,G) and (T,L) represent the generation and load at buses of transmission system, respectively. Also, $\Delta \mathbf{P}_B$ and $\Delta \mathbf{Q}_B$ are the change of real and reactive power references at the boundary buses, respectively. Then, the TSO is required to compare the FORs with the power references because their calculated values may be larger than the maximum powers, which each DSO can transmit. Suppose that the i -th DSO has the FOR of which the boundary is approximated by $f_i = 0$, and $(\Delta P_B^i$ and $\Delta Q_B^i)$ are calculated by (12), where P_B^i and Q_B^i are initial real and reactive power reference, respectively. Then, there are two possible cases depending on the FOR and new power reference, as shown in Fig. 4. In most cases, the point of new power reference at PQ -plane, $B_{\text{new}}^i (P_B^i + \Delta P_B^i, Q_B^i + \Delta Q_B^i)$, is within the boundary of FOR while satisfying $f_i (P_B^i + \Delta P_B^i, Q_B^i + \Delta Q_B^i) \leq 0$, as shown in Fig. 4(a). For this case, the TSO simply specifies the reference values to the DSOs. However, if the maximum power that the DSO can provide is small or a large fault occurs, $f_i (P_B^i + \Delta P_B^i, Q_B^i + \Delta Q_B^i)$ becomes greater than 0. This means that it locates outside the boundary of FOR, as shown in Fig. 4(b). In this case, the iterative computation is needed to ensure the optimality of control [35]. That is, the TSO must re-calculate the power references for the i -th DSO with $(\Delta P_{B,\text{update}}^i$ and $\Delta Q_{B,\text{update}}^i)$. They are obtained by solving the following optimization problem to minimize the distance between $B_{\text{new}}^i (P_B^i + \Delta P_B^i, Q_B^i + \Delta Q_B^i)$ and $B_{\text{update}}^i (P_B^i + \Delta P_{B,\text{update}}^i, Q_B^i + \Delta Q_{B,\text{update}}^i)$ at PQ -plane while satisfying $f_i = 0$ as

$$\min \left\{ (\Delta P_{B,\text{update}}^i - \Delta P_B^i)^2 + (\Delta Q_{B,\text{update}}^i - \Delta Q_B^i)^2 \right\} \quad (13)$$

$$\text{s.t. } f_i (P_B^i + \Delta P_{B,\text{update}}^i, Q_B^i + \Delta Q_{B,\text{update}}^i) = 0. \quad (14)$$

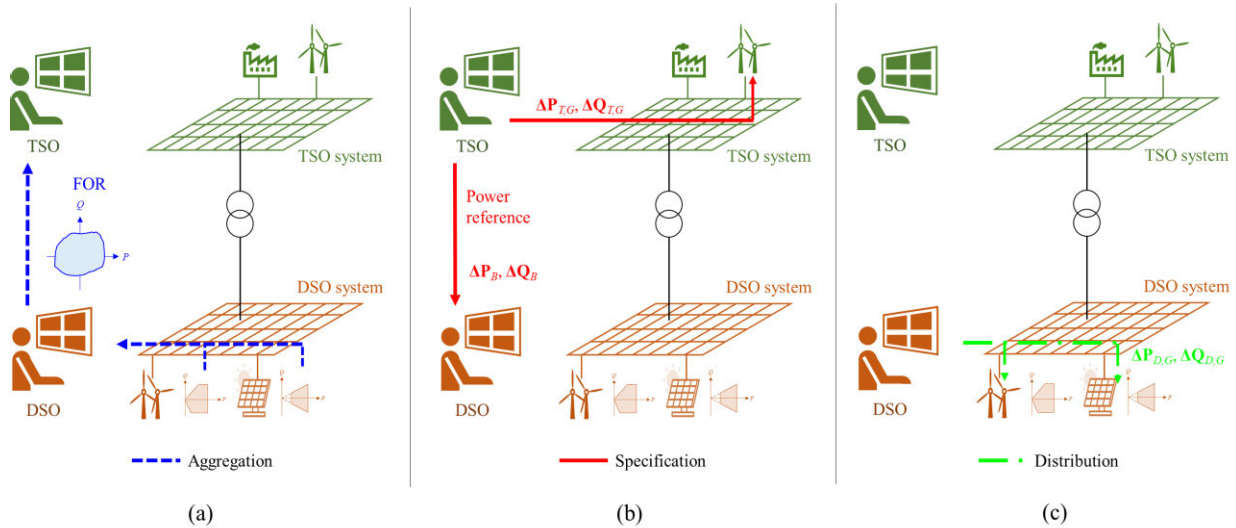


FIGURE 2. The framework of proposed three-step cooperative control process: (a) aggregation, (b) specification, (c) distribution.

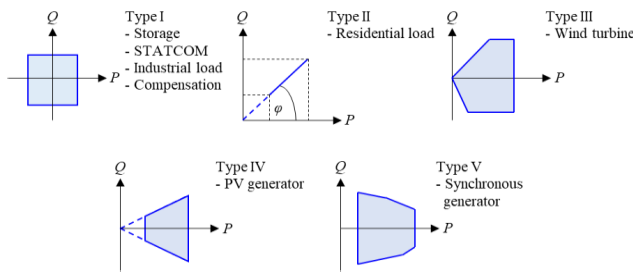


FIGURE 3. Five types of flexibility polygons of each DG at PQ-plane.

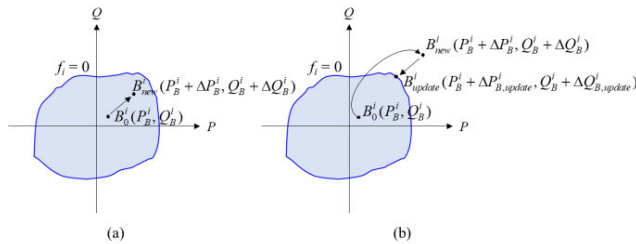


FIGURE 4. Two cases for specifying the power references: (a) $f_i(B_{new}^i) \leq 0$, (b) $f_i(B_{new}^i) > 0$.

After determining the updated power reference for the i -th DSO, the j -th DSO needs to make up for the difference. To allocate the power references most effectively, the difference in power goes to the DSO which is the most sensitive among the DSOs. Then, from the generation-load sensitivity analysis, the largest power generation is allocated to the most sensitive bus to the change. In other words, j can be defined as

$$j = \arg \max_n \left\{ (\Delta P_B^n)^2 + (\Delta Q_B^n)^2 \right\} \quad (15)$$

$$s.t. f_j(P_B^j + \Delta P_B^j, Q_B^j + \Delta Q_B^j) < 0. \quad (16)$$

The updated power reference for the j -th DSO is the sum of new power reference calculated by using (12) and the remaining power from the i -th DSO. When the j -th DSO needs to make up for a large amount of remaining power, it might be outside the boundary of the FOR, as shown in Fig. 4(b). For this case, the process to re-calculate the reference is repeated for the j -th DSO by solving the optimization problem in (13) again.

If a line congestion occurs, the power reference is modified to satisfy the branch flow limits [36]. In other words, the objective function minimizes the sum of distances between the modified power reference deviations ($\Delta P_{B,mod}^i, \Delta Q_{B,mod}^i$) and previous power reference deviations calculated in advance ($\Delta P_B^i, \Delta Q_B^i$) as (17)–(21), shown at the bottom of the next page, where P_{ij} and Q_{ij} are real and reactive powers of branch flow at line i - j , respectively. Also, S_{ij}^{max} is the branch flow limit at line i - j .

After completing the procedure to adjust the power references for all DSOs, the TSO sends them to each DSO and distributes the power of generators that can be operated as virtual slack by using $\Delta P_{T,G}$ and $\Delta Q_{T,G}$ in (12). The final step is the local distribution as shown in Fig. 2(c). On receiving the power reference at boundary bus from the TSO, each DSO calculates how to allocate the powers optimally between the DGs in the distribution system. For the i -th DSO, this can be carried out as

$$\begin{bmatrix} \Delta P_{D,G} \\ \Delta Q_{D,G} \end{bmatrix} = S_{DSO} \cdot \begin{bmatrix} \Delta P_{D,L} \\ \Delta P_B^i \\ \Delta Q_{D,L} \\ \Delta Q_B^i \end{bmatrix}, \quad (22)$$

where the subscripts (D,G) and (D,L) represent the generation and load at the buses of distribution system, respectively. Also, ΔP_B^i and ΔQ_B^i is the i -th element of vectors, ΔP_B and ΔQ_B , respectively. The TSO calculates the power references

for all distribution systems connected with the transmission system (these make up for the vectors, $\Delta \mathbf{P}_B$ and $\Delta \mathbf{Q}_B$). However, each DSO needs to receive one element (ΔP_B^i and ΔQ_B^i) corresponding to the distribution network.

The DSO manages the power generations between the DGs based on the same procedure, which is used to calculate the power references between the DSOs. Thus, the DSO identifies whether the power reference of i -th DG calculated by (22), $(P_{D,G}^i + \Delta P_{D,G}^i, Q_{D,G}^i + \Delta Q_{D,G}^i)$ is inside the flexibility area at PQ -plane as Fig. 4. If it is outside this area, the power reference is re-calculated by (13)–(16). Finally, the real and reactive powers are properly allocated to all generators in the TSO-DSO system. The overall flowchart of proposed cooperative control is shown in Fig. 5.

D. COMPUTATIONAL BURDEN OF PROPOSED COOPERATIVE CONTROL

To analyze the computational burden of proposed cooperative control, there are three issues to be considered. They are the calculation of FOR, re-calculation of power references, and computation of power sensitivity matrix.

The calculation of FOR is solved by using Minkowski sum, which is used for the aggregation of flexibility in many studies [37], [38], [39]. The Minkowski sum of two sets of position vectors, A and B in Euclidean space is formed by adding each vector in A to each vector in B as

$$A + B = \{a + b \mid a \in A, b \in B\} \quad (23)$$

In general, if two sets A and B are convex polygons in \mathbb{R}^2 , the implementation of Minkowski sum is straightforward. Then, the computational complexity for summing two convex flexibility polygons is $O(m + n)$, where m and n are the numbers of vertices of A and B , respectively [39]. Note that the flexibilities of DGs have been defined by the convex polygons in many DSO studies, as shown in Fig. 3. Therefore, the computational complexity of calculating FOR is $O(n)$, where n is the number of DGs. As the result, the calculation of FOR is not a big burden even in a practical system with many DGs.

The FOR is the result of summing the flexibility polygons of DGs, and it can be defined as the polygon in PQ -plane. Then, the power reference point is easily obtained by the optimization process to find the minimum distance from the FOR to this polygon [40]. The computational complexity for

calculating the distance from point to polygon depends on the order of the number of vertices [41]. As the result, the maximum computational complexity for re-calculating the power references is $O(n \cdot m)$, where n and m are the numbers of DGs and DSOs, respectively.

The calculation of power sensitivity matrix requires to take inverse of Jacobian matrix via the power flow analysis. In general, the computational complexity of inverse of $n \times n$ matrix is $O(n^3)$ when the Gaussian elimination method is used [42]. Considering the size of Jacobian matrix is proportional to n number of buses, the complexity of calculating the power sensitivity matrix is $O(n^3)$. Differently from the centralized control approach shown in Fig. 1(b) (which requires to calculate entire power sensitivity matrix of integrated TSO-all DSOs system at once), the proposed cooperative control can reduce the size of power sensitivity matrix much smaller by considering the required coordination between the TSO and each DSO separately, as shown in Fig. 1(c).

In summary, the proposed approach can effectively reduce the computational burden required for the cooperative coordination between TSO and DSOs when compared to a centralized control approach. Also, the communicational burden is low, because the data used in the protocols is the coordinates of FOR and the power references which are just simple numbers, and the entire algorithm is implemented without any training process.

III. EVALUATION OF PERFORMANCE

The performance of proposed cooperative control of TSO-DSO is evaluated by carrying out several case studies on the IEEE 39-bus test system in Fig. 6. It has 10 generators, 19 loads, and four DSO systems, which are connected at buses 2, 9, 17, and 22. As shown in Fig. 7, each DSO system consists of four modified IEEE 33-bus radial distribution systems. The first distribution system has 33 buses and 3 DGs (DG1, DG2, and DG3), which are connected to buses 2, 22, and 33, respectively. The DG1 and DG3 have the characteristic of flexibility polygons of Type I. On the other hand, the DG2 has that of Type III. The maximum real power output from each DG is 15 MW. The other radial distribution systems are the same as the first one.

For the proposed cooperative control of TSO-DSO, the TSO firstly calculates the sensitivity matrix of system by (10).

$$\min_{P_{B,mod}, Q_{B,mod}, V, \theta} \left(\sum_i \sqrt{(\Delta P_{B,mod}^i - \Delta P_B^i)^2 + (\Delta Q_{B,mod}^i - \Delta Q_B^i)^2} \right) \quad (17)$$

$$s.t. f_i(P_B^i + \Delta P_{B,mod}^i, Q_B^i + \Delta Q_{B,mod}^i) \leq 0, \quad (18)$$

$$P_{ij} = |V_i| |Y_{ij}| \{ |V_j| \cos(\delta_i - \delta_j) - |V_j| \cos(\theta_{ij} - \delta_i + \delta_j) \}, \quad (19)$$

$$Q_{ij} = |V_i| |Y_{ij}| \{ |V_j| \sin(\delta_j - \delta_i) - |V_j| \sin(\theta_{ij} - \delta_i + \delta_j) \}, \quad (20)$$

$$(P_{ij})^2 + (Q_{ij})^2 \leq (S_{ij}^{\max})^2. \quad (21)$$

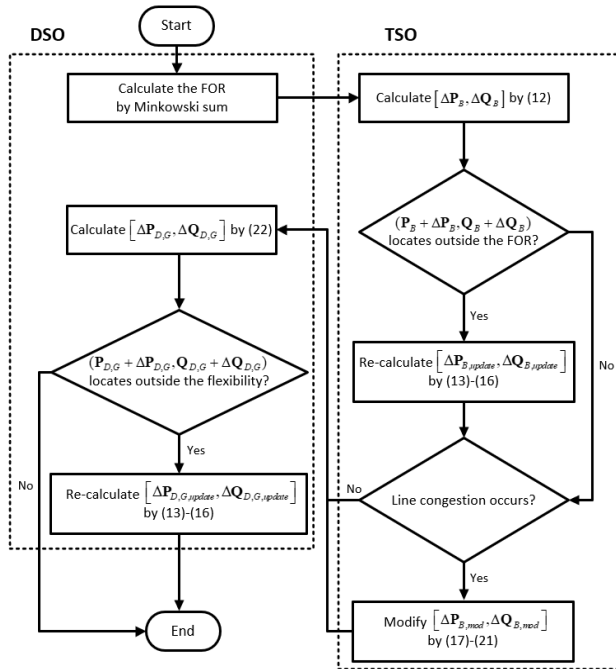


FIGURE 5. Flowchart of the proposed cooperative control of TSO-DSO.

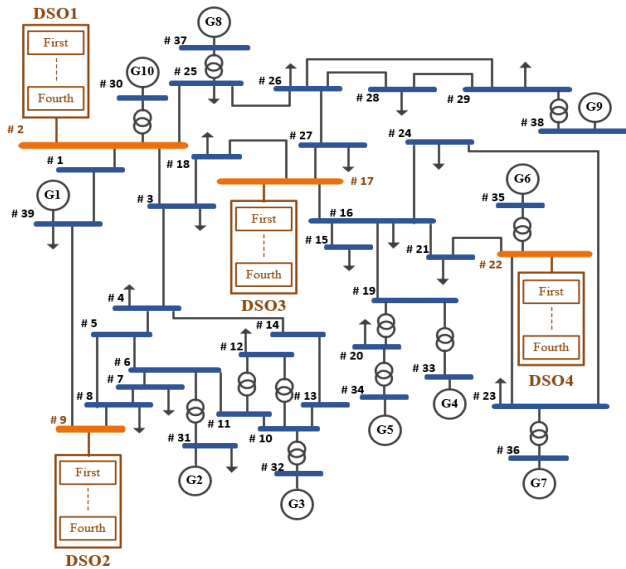


FIGURE 6. Single-line diagram of the IEEE 39-bus test system with four DSO systems.

The real power sensitivity heatmap, which visualizes the relationships between the systems of TSO and DSOs, is shown in Fig. 8. Note that there are no sensitivity elements at bus 31, which is a slack bus. This is because the power flow at the slack bus is not the target to be controlled. Thus, this corresponding sensitivity element is not needed. By using this heatmap, the TSO can figure out which DSO is electrically close to the buses of transmission system. As shown in Fig. 8, the DSO3 is electrically close to many buses with the relatively higher degree of real power sensitivity. In contrast, there are not many buses related to the DSO2 except for the bus 9, which is the boundary bus of DSO2.

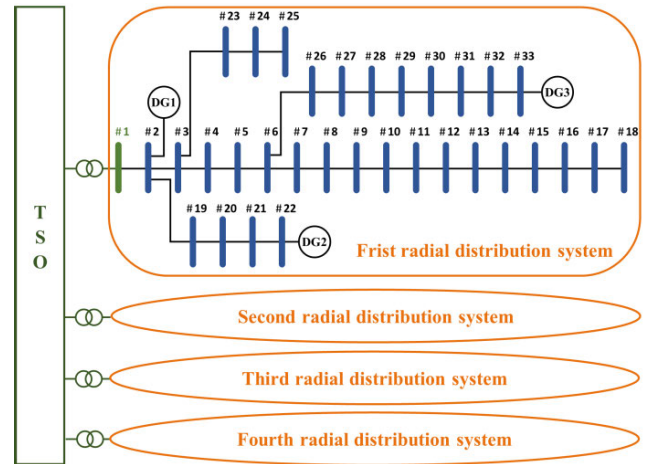


FIGURE 7. Single-line diagram of each DSO system with four modified IEEE 33-bus radial distribution systems.

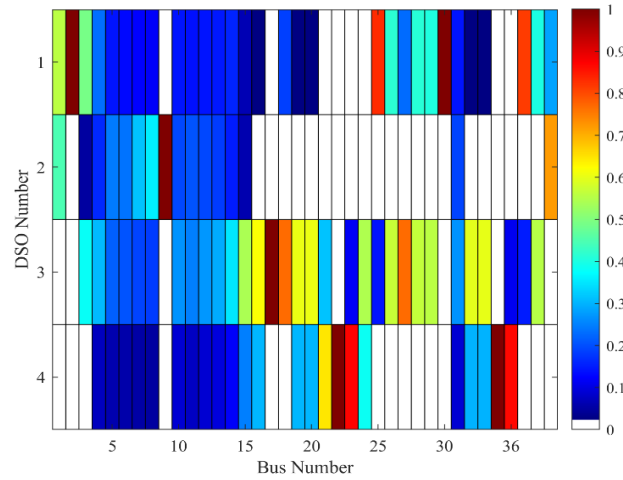


FIGURE 8. The real power sensitivity heatmap with respect to the relationship between the TSO and DSOs.

A. MANAGEMENT OF LINE CONGESTION

To verify the effectiveness of proposed cooperative control, the big load change is applied. In other words, it is assumed that the load demand at bus 39 in Fig. 6 is suddenly increased from 1104 MW to 1325 MW by 20%.

Note that the power references for four DSOs depend on the magnitudes of their power sensitivities in Fig. 8. For this case, they are larger in the order of (DSO2, DSO1, DSO4, and DSO3), as shown in Fig. 9, while indicating the point of power references and FORs at PQ -plane. The initial and new power references are marked with black and blue crosses, respectively.

It is clearly observed that all power references are inside their FORs. As the result, the new power references (B_{new}^1 , B_{new}^2 , B_{new}^3 , and B_{new}^4) calculated by using (12) are sent to all DSOs. After that, when the DSOs distribute their DGs, the power references for all DGs are calculated by using (22) again, while checking whether their power references are inside the flexibility areas of DGs at PQ -plane shown in Fig. 10, where they are marked with blue crosses. It is observed that these points are inside the flexibility areas of

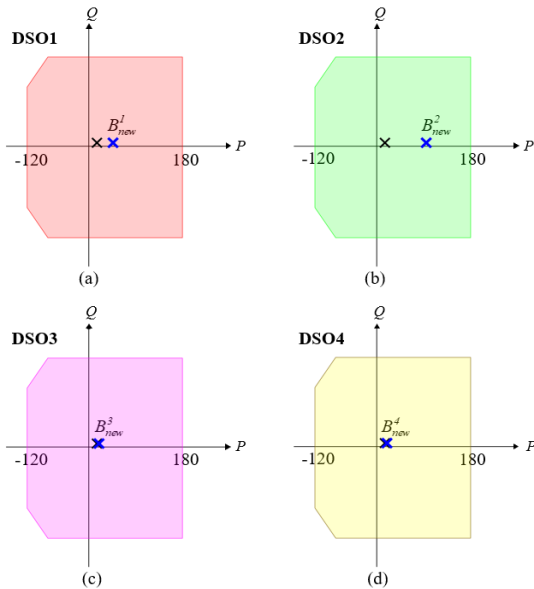


FIGURE 9. Power references and FORs of four DSOs when the load at bus 39 is suddenly increased: (a) DSO1, (b) DSO2, (c) DSO3, (d) DSO4.

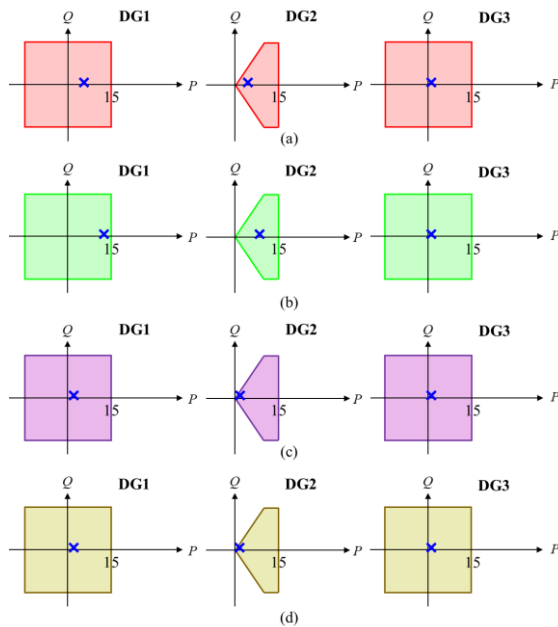


FIGURE 10. Power references and flexibility areas of DGs at the first radial distribution system when the load at bus 39 is suddenly increased: (a) DSO1, (b) DSO2, (c) DSO3, (d) DSO4.

DGs in the first radial system. The same results are obtained in the other radial systems. Thus, the DSO simply distributes the reference values as blue crosses.

Then, the results of line loadings at five transmission lines, which have high loading capacity after the load is increased, are given in Table 2.

It is observed that the serious transmission constraint problem occurs at line 21-22 with the loading capacity of 102.25%. This is because the power output from G6, which is close to line 21-22, is increased from 650 MW to 666 MW by 2.4%. In contrast, its loading capacity is reduced from

TABLE 2. Results of line loadings in TSO system.

Line	Before load is increased [%]	After load is increased	
		Without proposed control [%]	With proposed control [%]
21-22	99.08	102.25	98.97
16-19	81.90	85.14	81.73
5-6	76.22	77.93	76.16
6-7	71.88	79.09	71.69
10-11	61.43	67.09	61.27
Overall average	78.10	82.30	77.96

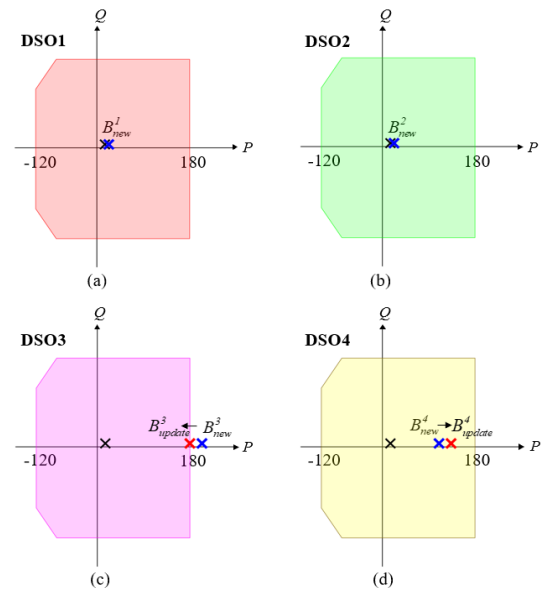


FIGURE 11. Power references and FORs of four DSOs when the G4 at bus 33 is suddenly disconnected: (a) DSO1, (b) DSO2, (c) DSO3, (d) DSO4.

99.08% to 98.97% by the proposed cooperative control method, by which the required powers are provided from the DSO1 and DSO2, while the power output from G6 is rather decreased very slightly from 650 MW to 649 MW. Moreover, overall average of line loading of 5 transmission lines is also decreased from 78.10% to 77.96%. This result clearly verifies that the line congestion problem is effectively handled by the proposed method.

B. FREQUENCY STABILITY FOR GENERATOR TRIP

To evaluate the effect of proposed method on frequency stability, the large generator, G4 at bus 33 in Fig. 6 is suddenly disconnected at 10 s. After this event occurs, the TSO firstly calculates the real power references for four DSOs. Again, they are related with the magnitude of their power sensitivities in Fig. 8. Then, their power references are larger in the order of (DSO3, DSO4, DSO1, and DSO2) for this case. The initial and new power references for four DSOs are marked with black and blue crosses, respectively, at PQ -plane in Fig. 11.

TABLE 3. Power outputs from generators in TSO system.

Generator	Before disconnection [MW]	At 30 s		
		Before applying control [MW]	<i>P</i> - <i>f</i> droop control [MW]	Proposed cooperative control [MW]
G1	1000	1274	1004	1002
G2	521	549	561	557
G3	650	685	680	680
G4	632	disconnected		
G5	508	529	510	510
G6	650	699	680	680
G7	560	601	595	595
G8	540	572	580	576
G9	830	888	850	850
G10	250	291	344	336
Total (TSO)	5509 (except for G4)	6088	5804	5786
Total (DSO)	60	60	358	358
Total (TSO+DSO)	5569	6148	6162	6144

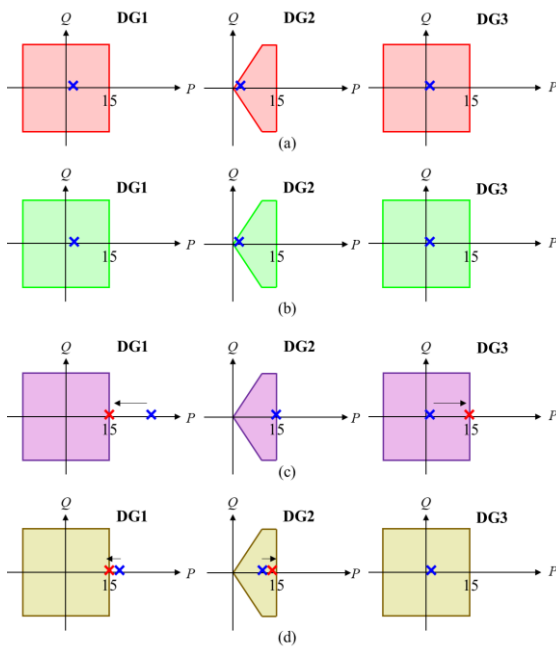


FIGURE 12. Power references and flexibility areas of DGs at the first radial distribution system when the G4 at bus 33 is suddenly disconnected: (a) DSO1, (b) DSO2, (c) DSO3, (d) DSO4.

It is observed that they are inside their FORs for the DSO1, DSO2, and DSO4. In contrast, the new power reference for the DSO3 is outside its FOR, as shown in Fig. 11(c). Therefore, its power reference must be re-calculated by using (13) and (14) so that it is placed in the FOR. Then, this updated reference for the DSO3 is marked with red cross.

Accordingly, the DSO4 takes the remaining power with its updated power reference based on the results from (15) and (16), as shown in Fig. 11(d). Finally, all power references ($B_{new}^1, B_{new}^2, B_{update}^3$, and B_{update}^4) are sent to the DSOs.

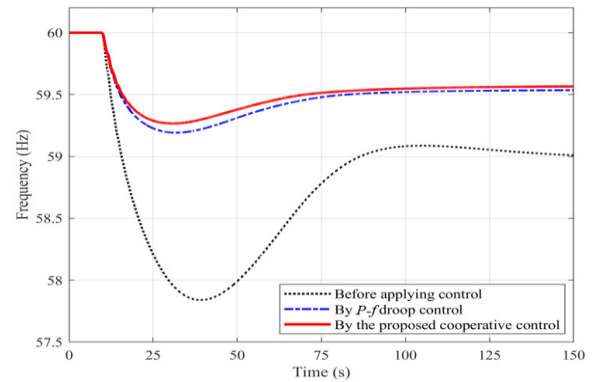


FIGURE 13. Frequency response when the generator G4 at bus 33 is suddenly dis-connected.

After that, when four DSOs distribute their DGs, the power references for all DGs are calculated by using (22) again, while identifying whether they are inside the flexibility areas of DGs at *PQ*-plane, as shown in Fig. 12.

They are initially marked with blue crosses. It is observed that the power references for the DSO1 and DSO2 are inside the flexibility areas of DGs. In contrast, the power references of DG1 in the DSO3 and DSO4 are outside the area, as shown in Figs. 12(c) and 12(d). Therefore, they are re-calculated by using (13) and (14) so that they are placed in the flexibility area at *PQ*-plane. Then, their updated power references are marked with red crosses. Then, for the DSO3, the DG3 is distributed with its updated power reference to take the remaining power from the DG1 based on the results from (15) and (16). Note that the power reference of DG2 is unchanged because it is already in the boundary of flexibility area, even though the DG2 has higher power sensitivity than the DG3. For the DSO4, the DG2 is distributed with its updated power reference for handling the remaining power. These updated

power references for the DG2 and DG3 are also marked with red crosses in Fig. 12(d).

When the G4 at bus 33 is suddenly disconnected at 10 s, the system frequency responses by the P - f droop control [43] and proposed cooperative control are compared in Fig. 13. The power outputs from conventional synchronous generators in the TSO system before the disconnection and at 30 s are given in Table 3. The frequency nadir and settling frequency become higher by two control methods, when compared to the case before taking any control actions. This is because the DGs of four DSOs generate more real powers after the system frequency drops. In particular, the frequency nadir by the proposed cooperative control is effectively increased than that by the P - f droop control, which is equally applied to all DGs. It is important to note that the total power generated from all DGs is the same for two control methods. However, the frequency response is improved by the proposed cooperative control. This is because the DSOs optimally distribute the DGs with higher power sensitivity such that they can generate more powers. Consequently, this result verifies that the proposed cooperative control can effectively improve the frequency stability of system.

Also, it is observed that the total amount of power outputs from all generators except for G4 in the TSO system is 5509 MW before the disconnection, as shown in Table 3. After the event occurs, it is increased to 6088 MW (without the control), 5804 MW (by the P - f droop control), and 5786 MW (by the proposed cooperative control) at 30 s. This means that all generators in the TSO system still support the frequency stability by increasing their power outputs in different amount after the disconnection of G4 for all cases. In particular, it is important to note that the total amount of power outputs from all generators in the TSO system is required the smallest by the proposed cooperative control, even though the sum of generations from all DGs is same by two control methods.

IV. CONCLUSION

This study proposed a new cooperative control method of transmission system operator (TSO) and distribution system operator (DSO) in power system based on the generation-load power sensitivity analysis. For the cooperative control, the DSOs aggregated the flexibility areas of distributed generators (DGs) in their networks and sent the feasible operation regions (FORs) to the TSO. After receiving the FORs, the TSO calculated the power references at the boundary buses between the transmission and distribution systems. Then, the DSOs took these references as loads to calculate the detailed power references for their DGs. As the result, the DSO could distribute the DGs effectively in response to several changes. Finally, the system response was improved by allocating power generation properly among the generators for the TSO-DSO.

To verify the effectiveness of proposed cooperative control, several case studies were carried out on the modified IEEE test system. The results showed that the power imbalances

caused by a sudden load change or generator trip can be effectively handled by all generators located in the TSO-DSO system, while successfully managing line congestion and frequency stability problems.

REFERENCES

- [1] D. Agdas and P. Barooh, "Impact of the COVID-19 pandemic on the U.S. electricity demand and supply: An early view from data," *IEEE Access*, vol. 8, pp. 151523–151534, 2020.
- [2] I. Tsiropoulos, W. Nijs, D. Tarvydas, and P. R. Castello, "Towards net-zero emissions in the EU energy system by 2050," Office Eur. Union, Luxembourg, U.K., Tech. Rep. EUR 29981 EN, 2020, doi: 10.2760/062347.
- [3] H. C. Lau and S. C. Tsai, "Global decarbonization: Current status and what it will take to achieve net zero by 2050," *Energies*, vol. 16, no. 23, p. 7800, Nov. 2023.
- [4] A. C. Serban and M. D. Lytras, "Artificial intelligence for smart renewable energy sector in Europe—Smart energy infrastructures for next generation smart cities," *IEEE Access*, vol. 8, pp. 77364–77377, 2020.
- [5] D. Ortiz-Villalba, C. Rahmann, R. Alvarez, C. A. Canizares, and C. Strunck, "Practical framework for frequency stability studies in power systems with renewable energy sources," *IEEE Access*, vol. 8, pp. 202286–202297, 2020.
- [6] T. Soares, "Renewable energy sources offering flexibility through electricity markets," Ph.D. dissertation, Dept. Elect. Eng., Tech. Univ. Denmark, Kongens Lyngby, Denmark, 2017.
- [7] M. Mousavi and M. Wu, "ISO and DSO coordination: A parametric programming approach," in *Proc. IEEE Power Energy Soc. Gen. Meeting (PESGM)*, Jul. 2022, pp. 1–5.
- [8] J. Silva, J. Sumaili, R. J. Bessa, L. Seca, M. A. Matos, V. Miranda, M. Caujolle, B. Goncer, and M. Sebastian-Viana, "Estimating the active and reactive power flexibility area at the TSO-DSO interface," *IEEE Trans. Power Syst.*, vol. 33, no. 5, pp. 4741–4750, Sep. 2018.
- [9] J. Cochran, M. Miller, M. Milligan, E. Ela, D. Arent, A. Bloom, M. Futch, J. Kiviluoma, H. Holtinnen, E. Gómez-Lázaro, S. Martín-Martínez, S. Kukoda, G. Garcia, K. M. Mikkelsen, Z. Yongqiang, and K. Sandholt, "Market evolution: Wholesale electricity market design for 21st century power system," Clean Energy Ministerial, Golden, CO, USA, Tech. Rep. NREL/TP-6A20-57477, Oct. 2013.
- [10] P. Cuffe, P. Smith, and A. Keane, "Transmission system impact of wind energy harvesting networks," *IEEE Trans. Sustain. Energy*, vol. 3, no. 4, pp. 643–651, Oct. 2012.
- [11] M. I. Alizadeh, M. Usman, F. Capitanescu, and A. G. Madureira, "A novel TSO-DSO ancillary service procurement coordination approach for congestion management," in *Proc. IEEE Power Energy Soc. Gen. Meeting (PESGM)*, Jul. 2022, pp. 1–5.
- [12] H. Sun, Q. Guo, B. Zhang, Y. Guo, Z. Li, and J. Wang, "Master-slave-splitting based distributed global power flow method for integrated transmission and distribution analysis," *IEEE Trans. Smart Grid*, vol. 6, no. 3, pp. 1484–1492, May 2015.
- [13] A. Kargarian and Y. Fu, "System of systems based security-constrained unit commitment incorporating active distribution grids," *IEEE Trans. Power Syst.*, vol. 29, no. 5, pp. 2489–2498, Sep. 2014.
- [14] Z. Li, Q. Guo, H. Sun, and J. Wang, "Coordinated economic dispatch of coupled transmission and distribution systems using heterogeneous decomposition," *IEEE Trans. Power Syst.*, vol. 31, no. 6, pp. 4817–4830, Nov. 2016.
- [15] R. Roofegari nejad, W. Sun, and A. Golshani, "Distributed restoration for integrated transmission and distribution systems with DERs," *IEEE Trans. Power Syst.*, vol. 34, no. 6, pp. 4964–4973, Nov. 2019.
- [16] Z. Li, J. Wang, H. Sun, and Q. Guo, "Transmission contingency analysis based on integrated transmission and distribution power flow in smart grid," *IEEE Trans. Power Syst.*, vol. 30, no. 6, pp. 3356–3367, Nov. 2015.
- [17] Z. Li, Q. Guo, H. Sun, J. Wang, Y. Xu, and M. Fan, "A distributed transmission-distribution-coupled static voltage stability assessment method considering distributed generation," *IEEE Trans. Power Syst.*, vol. 33, no. 3, pp. 2621–2632, May 2018.
- [18] H. Jia, W. Qi, Z. Liu, B. Wang, Y. Zeng, and T. Xu, "Hierarchical risk assessment of transmission system considering the influence of active distribution network," *IEEE Trans. Power Syst.*, vol. 30, no. 2, pp. 1084–1093, Mar. 2015.

- [19] A. Mohammadi, M. Mehrdash, and A. Kargarian, "Diagonal quadratic approximation for decentralized collaborative TSO+DSO optimal power flow," *IEEE Trans. Smart Grid*, vol. 10, no. 3, pp. 2358–2370, May 2019.
- [20] D. A. Contreras and K. Rudion, "Computing the feasible operating region of active distribution networks: Comparison and validation of random sampling and optimal power flow based methods," *IET Gener., Transmiss. Distrib.*, vol. 15, no. 10, pp. 1600–1612, May 2021.
- [21] J. M. Morales, S. Pineda, and Y. Dvorkin, "Learning the price response of active distribution networks for TSO-DSO coordination," *IEEE Trans. Power Syst.*, vol. 37, no. 4, pp. 2858–2868, Jul. 2022.
- [22] M. Sarstedt and L. Hofmann, "Monetization of the feasible operation region of active distribution grids based on a cost-optimal flexibility disaggregation," *IEEE Access*, vol. 10, pp. 5402–5415, 2022.
- [23] A. Singhal, A. K. Bharati, and V. Ajjarapu, "Deriving DERs VAR-capability curve at TSO-DSO interface to provide grid services," *IEEE Trans. Power Syst.*, vol. 38, no. 2, pp. 1820–1833, Mar. 2023.
- [24] H. Bakhtiari, M. R. Hesamzadeh, and D. Bunn, "TSO-DSO operational coordination using a look-ahead multi-interval framework," *IEEE Trans. Power Syst.*, vol. 38, no. 5, pp. 4221–4239, Sep. 2023.
- [25] D. Choi, J.-W. Park, and S. H. Lee, "Virtual multi-slack droop control of stand-alone microgrid with high renewable penetration based on power sensitivity analysis," *IEEE Trans. Power Syst.*, vol. 33, no. 3, pp. 3408–3417, May 2018.
- [26] M. Tostado-Véliz, T. Alharbi, O. Alrumayh, S. Kamel, and F. Jurado, "A novel power flow solution paradigm for well and ill-conditioned cases," *IEEE Access*, vol. 9, pp. 112425–112438, 2021.
- [27] F. Milano, "Analogy and convergence of Levenberg's and Lyapunov-based methods for power flow analysis," *IEEE Trans. Power Syst.*, vol. 31, no. 2, pp. 1663–1664, Mar. 2016.
- [28] S. Kar, G. Hug, J. Mohammadi, and J. M. F. Moura, "Distributed state estimation and energy management in smart grids: A consensus+ innovations approach," *IEEE J. Sel. Topics Signal Process.*, vol. 8, no. 6, pp. 1022–1038, Dec. 2014.
- [29] R. Scherdfeger, S. Schlegel, D. Westermann, M. Lutter, and M. Jung-Hans, "Methodology for next generation system operation between DSO and DSO," CIGRE Study Committee C2, SC C2 Syst. Operation Control, Paris, France, White Paper C2-207, 2016.
- [30] M. Sarstedt, L. Kluß, M. Dokus, L. Hofmann, and J. Gerster, "Simulation of hierarchical multi-level grid control strategies," in *Proc. Int. Conf. Smart Grids Energy Syst. (SGES)*, Nov. 2020, pp. 175–180.
- [31] D. A. Contreras and K. Rudion, "Improved assessment of the flexibility range of distribution grids using linear optimization," in *Proc. Power Syst. Comput. Conf. (PSCC)*, Jun. 2018, pp. 1–7.
- [32] D. A. Contreras and K. Rudion, "Time-based aggregation of flexibility at the TSO-DSO interconnection point," in *Proc. IEEE Power Energy Soc. Gen. Meeting (PESGM)*, Aug. 2019, pp. 1–5.
- [33] A. Patig, O. Stanojev, P. Aristidou, A. Kiprakis, and G. Hug, "Fast mapping of flexibility regions at TSO-DSO interfaces under uncertainty," in *Proc. IEEE PES Innov. Smart Grid Technol. Conf. Eur. (ISGT-Europe)*, Oct. 2022, pp. 1–6.
- [34] L. Roald and G. Andersson, "Chance-constrained AC optimal power flow: Reformulations and efficient algorithms," *IEEE Trans. Power Syst.*, vol. 33, no. 3, pp. 2906–2918, May 2018.
- [35] H. Qiu, B. Zhao, W. Gu, and R. Bo, "Bi-level two-stage robust optimal scheduling for AC/DC hybrid multi-microgrids," *IEEE Trans. Smart Grid*, vol. 9, no. 5, pp. 5455–5466, Sep. 2018.
- [36] D. A. Contreras, S. Müller, and K. Rudion, "Congestion management using aggregated flexibility at the TSO-DSO interface," in *Proc. IEEE Madrid PowerTech*, Jun. 2021, pp. 1–6.
- [37] S. Barot and J. A. Taylor, "A concise, approximate representation of a collection of loads described by polytopes," *Int. J. Electr. Power Energy Syst.*, vol. 84, pp. 55–63, Jan. 2017.
- [38] S. You, J. Hu, and C. Ziras, "An overview of modeling approaches applied to aggregation-based fleet management and integration of plug-in electric vehicles," *Energies*, vol. 9, no. 11, p. 968, Nov. 2016.
- [39] E. Fogel, D. Halperin, and C. Weibel, "On the exact maximum complexity of Minkowski sums of polytopes," *Discrete Comput. Geometry*, vol. 42, no. 4, pp. 654–669, Dec. 2009.
- [40] T. Long and W. Jiao, "The geometric correction model based on areal features for multisource images rectification," *Int. Arch. Photogramm., Remote Sens. Spatial Inf. Sci.*, vol. XXXIX-B1, pp. 245–249, Jul. 2012.
- [41] L. Lenarduzzi, "Compression of corneal maps of curvature," *Appl. Math. Comput.*, vol. 252, pp. 77–87, Feb. 2015.

- [42] J. von zur Gathen and J. Gerhard, *Modern Computer Algebra*. Cambridge, U.K.: Cambridge Univ. Press, 2003.
- [43] S. D'Arco and J. A. Suul, "Equivalence of virtual synchronous machines and frequency-droops for converter-based MicroGrids," *IEEE Trans. Smart Grid*, vol. 5, no. 1, pp. 394–395, Jan. 2014.



KIYO YOON (Member, IEEE) received the B.S. and Ph.D. degrees from the Department of Electrical Engineering, Yonsei University, Seoul, South Korea, in 2017 and 2023, respectively. He is currently a Postdoctoral Research Associate with the School of Electrical and Electronic Engineering, Yonsei University. His research interests include TSO-DSO coordination and power system stability.



JOOHYUK LEEM (Student Member, IEEE) received the B.S. degree from the Department of Electrical Engineering and Computer Science, University of Tennessee, Knoxville, TN, USA, in 2019. He is currently pursuing the Ph.D. degree through the combined M.S. and Ph.D. Program with the School of Electrical and Electronic Engineering, Yonsei University, Seoul, South Korea. His research interests include TSO-DSO coordination and power system stability.



SOO HYOUNG LEE (Member, IEEE) received the B.S. and Ph.D. degrees in electrical engineering from the School of Electrical and Electronic Engineering, Yonsei University, Seoul, South Korea, in 2008 and 2012, respectively. He was a Postdoctoral Research Associate with the School of Electrical and Computer Engineering, Georgia Institute of Technology, Atlanta, GA, USA, from 2012 to 2014. He was a Senior Researcher with the Advanced Power Grid Research Division, Korea Electrotechnology Research Institute, Uiwang-si, South Korea, from 2014 to 2018. He was an Assistant Professor with the Department of Electrical and Control Engineering, Mokpo National University, Muan, South Korea, from 2018 to 2023. He is currently an Assistant Professor with the Division of Electrical, Electronic and Control Engineering, Kongju National University, Cheonan-si, South Korea. His research interests include converter-based microgrids, the optimal coordination of distributed generation systems, and converter control for distributed generation systems.



JUNG-WOOK PARK (Senior Member, IEEE) was born in Seoul, South Korea. He received the B.S. degree (summa cum laude) from the Department of Electrical Engineering, Yonsei University, Seoul, in 1999, and the M.S.E.C.E. and Ph.D. degrees from the School of Electrical and Computer Engineering, Georgia Institute of Technology, Atlanta, GA, USA, in 2000 and 2003, respectively. From 2003 to 2004, he was a Postdoctoral Research Associate with the Department of Electrical and Computer Engineering, University of Wisconsin-Madison, Madison, WI, USA. Since 2005, he has been with the School of Electrical and Electronic Engineering, Yonsei University, where he is currently a Professor. His current research interests include power system dynamics, energy management systems, renewable energies-based distributed generation systems, and the hardware implementation of power electronics-based inverters.